How ocean color can steer Pacific tropical cyclones

Anand Gnanadesikan,[1] Kerry Emanuel,[2] Gabriel A. Vecchi,[1] Whit G. Anderson,[1] and Robert Hallberg[1]

[1] Because ocean color alters the absorption of sunlight, it can produce changes in sea surface temperatures with further impacts on atmospheric circulation. These changes can project onto fields previously recognized to alter the distribution of tropical cyclones. If the North Pacific subtropical gyre contained no absorbing and scattering materials, the result would be to reduce subtropical cyclone activity in the subtropical Northwest Pacific by 2/3, while concentrating cyclone tracks along the equator. Predicting tropical cyclone activity using coupled models may thus require consideration of the details of how heat moves into the upper thermocline as well as biogeochemical cycling. **Citation:** Gnanadesikan, A., K. Emanuel, G. A. Vecchi, W. G. Anderson, and R. Hallberg (2010), How ocean color can steer Pacific tropical cyclones, *Geophys. Res. Lett.*, *37*, L18802, doi:10.1029/2010GL044514.

1. Introduction

[2] Models of ocean solar heating calibrated against in-situ data [e.g., *Morel*, 1988; *Lewis et al.*, 1990; *Manizza et al.*, 2005] predict that in perfectly clear water a downwelling surface shortwave flux of 200W/m^2 would lead to a heating rate of ~0.75 C/yr at 100m, while at 200m the rate would be ~0.07 C/yr. However, because scattering and absorbing materials in seawater affect the degree to which sunlight penetrates into the ocean interior, the heating rate is generally much smaller. Chlorophyll-dependent parameterizations of shortwave heating show that even in waters that are relatively clear much of this heating is blocked, so that waters below about 100m can be significantly cooled by the presence of ocean color. Isolating the effect of such solar heating changes in nature is difficult, as temporal variations in both temperature and chlorophyll are affected by mixing and advection. Model studies have shown that, in isolation, alteration of the heating profile can alter sea surface temperatures (SSTs) in the tropics [*Nakamoto et al.*, 2001; *Manizza et al.*, 2005; *Lengaigne et al.*, 2007], especially in the Pacific basin [*Sweeney et al.*, 2005; *Anderson et al.*, 2007; *Gnanadesikan and Anderson*, 2009].

[3] This paper evaluates whether such SST changes can change the climatology of tropical cyclones (TCs), particularly in the North Pacific. Variation in the occurrence, intensity, duration and paths of TCs have been tied to the El Nino Southern Oscillation [*Chan*, 1985; *Saunders et al.*,

2000; *Camargo et al.*, 2007]. Models are able to recover these interannual variations [*Zhao et al.*, 2009] suggesting that they are strongly controlled by large-scale environmental conditions. Using two downscaling techniques, this paper demonstrates that changes in surface temperatures and tropical circulation caused by including chlorophyll-dependent solar heating have a first-order impact on the spatiotemporal distribution of TCs.

2. Methods

2.1. Background SST and Atmospheric Circulation Changes due to Ocean Color

[4] The impact of chlorophyll-dependent solar heating on the background tropical circulation was evaluated using coupled climate models. The atmospheric, land, and sea ice components were taken from GFDL's CM2.1 global coupled climate model [*Delworth et al.*, 2006], one of the most skillful climate simulations in the IPCC Fourth Assessment report [*Reichler and Kim*, 2008]. However, in order to minimize spurious numerical diffusion in the upper thermocline which would lead to smoothing out the impacts of heating perturbations [*Griffies et al.*, 2000], an isopycnal ocean model [*Hallberg and Gnanadesikan*, 2006] was used. The new coupled model simulates ocean hydrography better than the CM2.1 model, though errors in SST are somewhat worse [*Gnanadesikan and Anderson*, 2009]. It also has a mechanistically realistic El Nino [*Anderson et al.*, 2009].

[5] Our initial set of simulations builds on the work of *Gnanadesikan and Anderson* [2009] to isolate the *total* impact of chlorophyll-dependent solar heating, with a focus on the Northwest Pacific. The control (Green) simulation in these runs used a chlorophyll-dependent solar heating parameterization with one band of penetrating radiation, in which the solar heating rate within the water column is given by

$$Q = 0.21 I_{sw} k_{bg} \exp(-k_{bg}z)$$
$$k_{bg} = 0.0232 + 0.064 * chl^{0.674} \tag{1}$$

Where I_{sw} is the incoming shortwave radation and *chl* is the chlorophyll concentration in mg/m^3. The Green run uses a monthly climatological surface chlorophyll concentration taken from the SeaWiFS satellite [*Yoder and Kennelly*, 1996]. As this parameterization does not include the impact of a deep chlorophyll maximum, it represents a *lower* limit on the total impact of chlorophyll-dependent absorption. Removing all color will generally represent a bigger perturbation than is seen here.

[6] We focus on a perturbation run (BLPGyre) where chl was set to zero in the Pacific within 30 degrees of the equator when concentrations dropped below 0.2 mg/m^3

[1]Geophysical Fluid Dynamics Laboratory, NOAA, Princeton, New Jersey, USA.
[2]Department of Earth, Atmosphere and Planetary Sciences, Massachusetts Institute of Technology, Cambridge, Massachusetts, USA.

(a) TC Frequency (days/yr/5 deg bin)   (b) GPI, Control   (c) TC Frequency from Downscaling, Control
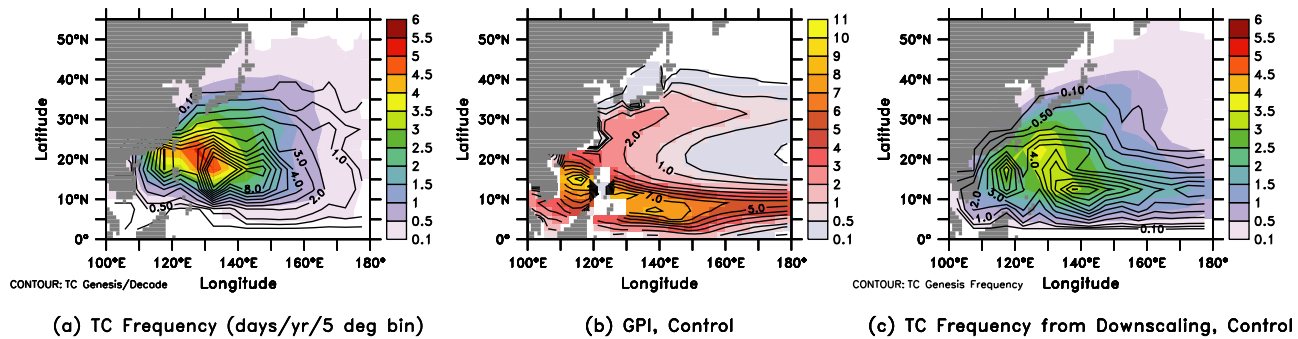
Figure 1. Cyclogenesis in the western North Pacific. (a) Observed TC days/year (one TC day means an entire day with a tropical storm within a 5 degree bin) from 1945–2008 and genesis within a five degree-bin/decade. Dataset compiled from NOAA Tropical Prediction Center for the North Atlantic and Eastern North Pacific and the Navy Joint Typhoon Warning Center for the rest of the globe. Available at ftp://texmex.mit.edu/pub/emanuel/HURR/tracks/). (b) Genesis Potential Index from control run. (c) TC frequency (days/yr/5 degree bin colors), and genesis frequency (storms/decade/5 degree bin contours), using the statistical-dynamical downscaling with environmental conditions given by control run.

(shown by the hatching in Figure 2a). This value was chosen because it represents an e-folding depth of ~23m, close to the value often used for the clearest waters [*Jerlov*, 1968] and because it has been used to represent the boundary between the gyre edge and upwelling/subtropical biomes [*Schultz*, 2008]. We will also refer to a simulation where chlorophyll concentrations were reduced by 50% globally (Half). While such perturbations are large, they are chosen to isolate and put reasonable bounds on the total potential impact of ocean color.

2.2. Impact on TC Formation

[7] The impact of SST changes on TC activity is estimated in two ways. The first is an empirically-derived Genesis Potential Index (GPI) relating environmental conditions to the number of TCs found in different regions. Following *Camargo et al.* [2007]

$$GPI = (PI/70)^3 \times (1 + 0.1*|U_{200} - U_{850}|)^{-2} \times (RH_{700}/50)^3 \times (Vort_{850} \times 10^5)^{3/2} \qquad (2)$$

In this formula PI is the potential intensity. U_{200}-U_{850} is the shear of the zonal wind between the 200 mb and 850 mb in m/s, RH_{700} is the relative humidity at 700mb in percent and $Vort_{850}$ is the absolute vorticity (curl of the vector horizontal wind + Coriolis parameter) at 850mb in s^{-1}.

[9] PI is based on a line of theoretical papers (starting with *Emanuel* [1986]) linking the dynamics and thermodynamics of TCs. Serving as a measure of the thermodynamic disequilibrium between the ocean and atmosphere, it represents the peak intensity the storm can attain under ideal conditions. GPI builds upon the PI, accounting for the effects of vorticity in creating conditions that are more favorable for convective organization, shear in preventing such organization, and low relative humidity in the middle of the atmosphere in inhibiting storm formation and maintenance. GPI has been used to evaluate changes in cyclogenesis associated with ENSO [*Camargo et al.*, 2007], intraseasonal oscillations [*Camargo et al.*, 2009] and climate change [*Vecchi and Soden*, 2007].

[10] Focusing on the northwest Pacific, the observed distribution of genesis (contours, Figure 1a) shows a region

with high levels of genesis between 120–150E and 10–20N. The Northwest Pacific experiences an average of 131 "TC days" each year; vs. 61 for the Atlantic and 58 for the Northeast Pacific. It accounts for 55% of reported hurricane-force winds over the past 25 years [*Maue*, 2009] with the region of maximum storminess lying to the northwest of the high-genesis region. The GPI in our control run (Figure 1b) captures the magnitude of cyclogenesis, with a band in which 8–9 storms are generated per decade in a given 5° bin. The location of this band, however is offset equatorward by 5–10°, most likely indicating biases in the modeled atmospheric circulation (a similar bias is found in other basins for Green run, but other configurations of our coupled model show the opposite bias).

[11] The second technique is the statistical-dynamical downscaling of *Emanuel* [2006]. This technique involves randomly seeding the tropics with weak, warm-core vortices that are then advected by the large-scale steering flow. The steering flow consists of synthetic time series of winds at two levels whose monthly mean, variances, and covariances are those of the coupled model. The result is to produce an ensemble of paths which track through spatially-varying environmental conditions. The resulting paths and environmental conditions are used to drive a simple radially symmetric, coupled atmosphere-ocean model to predict the intensity and size of the cyclone that develops. The vast majority of vortices do not develop into hurricane-strength storms. This approach neglects the possibility that changes in the climatology of the triggering disturbances (rather than the development of these disturbances) could be responsible for variability in tropical cyclogenesis. The predicted distribution of cyclones in our Green control run (Figure 1c) reproduces the pattern of TC frequency (correlation coefficient of 0.89) and TC genesis (correlation coefficient of 0.72) and a slight equatorward bias.

3. Results

[12] As seen in Figure 2, increasing the penetration depth of solar radiation from >23m (Green) to ~40m (BLPGyre) in the low-chlorophyll subtropical gyres changes several components of the GPI. SSTs in the gyres drop and subsurface waters warm, with a small part of this deep heating carried to
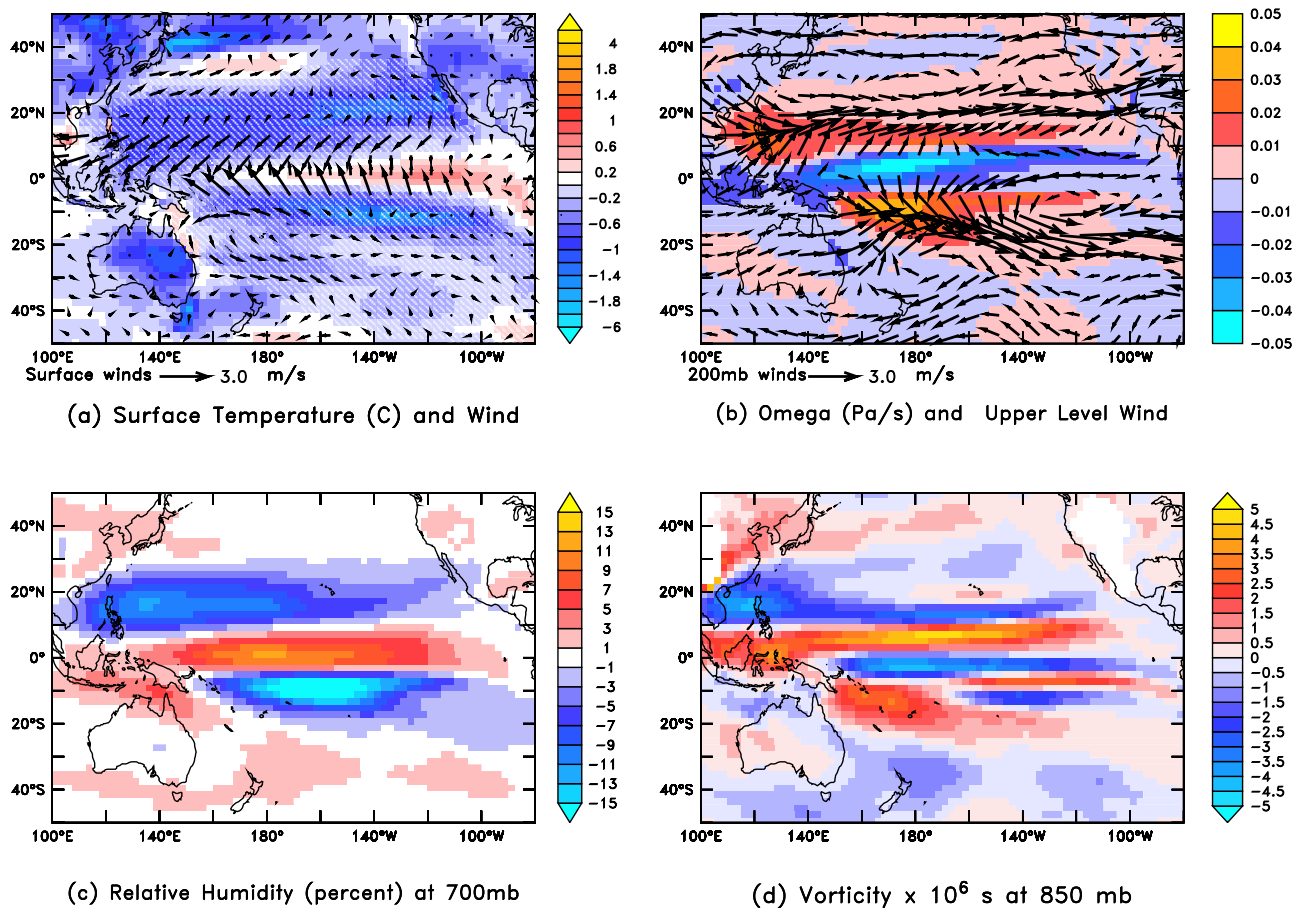
Figure 2. Changes in environmental conditions brought about by removing color-dependent absorption from low-chlorophyll regions in the subtropical gyres (shown by hatching in Figure 2a) in a coupled climate model. All fields are annual averages from years 41–120. Since changes in these fields tend to be more extreme in the summer season, the impact on TC formation will in general be more pronounced than would be inferred from these plots. (a) Changes in surface temperature in degrees (colors) and 2m winds (vectors). (b) Changes in vertical velocity at 500m in pressure units of Pa/s (colors) and upper level winds at 200mb (vectors). (c) Changes in relative humidity at 700mb. (d) Changes in vorticity (curl of the horizontal velocity) at 850mb. In northern hemisphere, positive vorticity values are associated with lower pressures, while in the southern hemisphere the opposite is true.

the equator on decadal timescales [*Gnanadesikan and Anderson*, 2009]. This pattern of SST change (Figure 2a) leads to a strengthening of the atmospheric Hadley circulation, with flow from the strong cold to the weak warm anomaly (vectors, Figure 2a). The resulting upward motion and precipitation along the Equator increases outflow aloft (Figure 2b). As the outflow moves away from the equator it is turned eastward by the Coriolis force, producing higher westerly winds. Intensification of the sinking branch of the Hadley circulation (Figure 2b) transports more dry air into the lower troposphere, causing both a reduction in relative humidity (Figure 2c) and, by compressing the air column, decreasing its cyclonic vorticity (Figure 2d).

[13] The GPI in the BLPGyre run drops over the subtropical zones relative to the Green control but increases in the near-equatorial region (Figure 3a). We can evaluate which of the changes in Figure 2 are most important to the total change in TC activity by replacing each component of the GPI separately. In the off-equatorial region (Figure 3b), a 70% total drop in genesis potential involves contributions from all four factors. Wind shear appears to be the largest of

these, followed by potential intensity and relative humidity, with vorticity playing a small role.

[14] The statistical-dynamical downscaling technique shows a similar shift in TC frequency and genesis (Figure 3c) The tracks in the BLPGyre run are much more focused near the equator, with more storms tracking into the South China Sea, but virtually no tracks moving into the East China Sea and many fewer landfalls in Japan and South China. The changes in genesis are roughly the same magnitude as those predicted by the GPI. Zonally averaged changes in TC frequency (Figure 3d), show an increase in the equatorial zones, and a decrease approaching 60% in the higher latitudes. This decrease is more pronounced for typhoons (max winds > 33 m/s) than for all TCs; implying that not only the location but the intensity of TCs is affected by the presence of ocean color.

[15] As described by *Anderson et al.* [2009] removing ocean color in the gyres can also impact tropical variability, so that interannual SST variance in the NINO3 region (180W–90W, 5N–5S) in the BLPGyre run is only 40% of that in the Green run. To what extent does this affect cyclone variability? The number of cyclone days (Figure 4a)
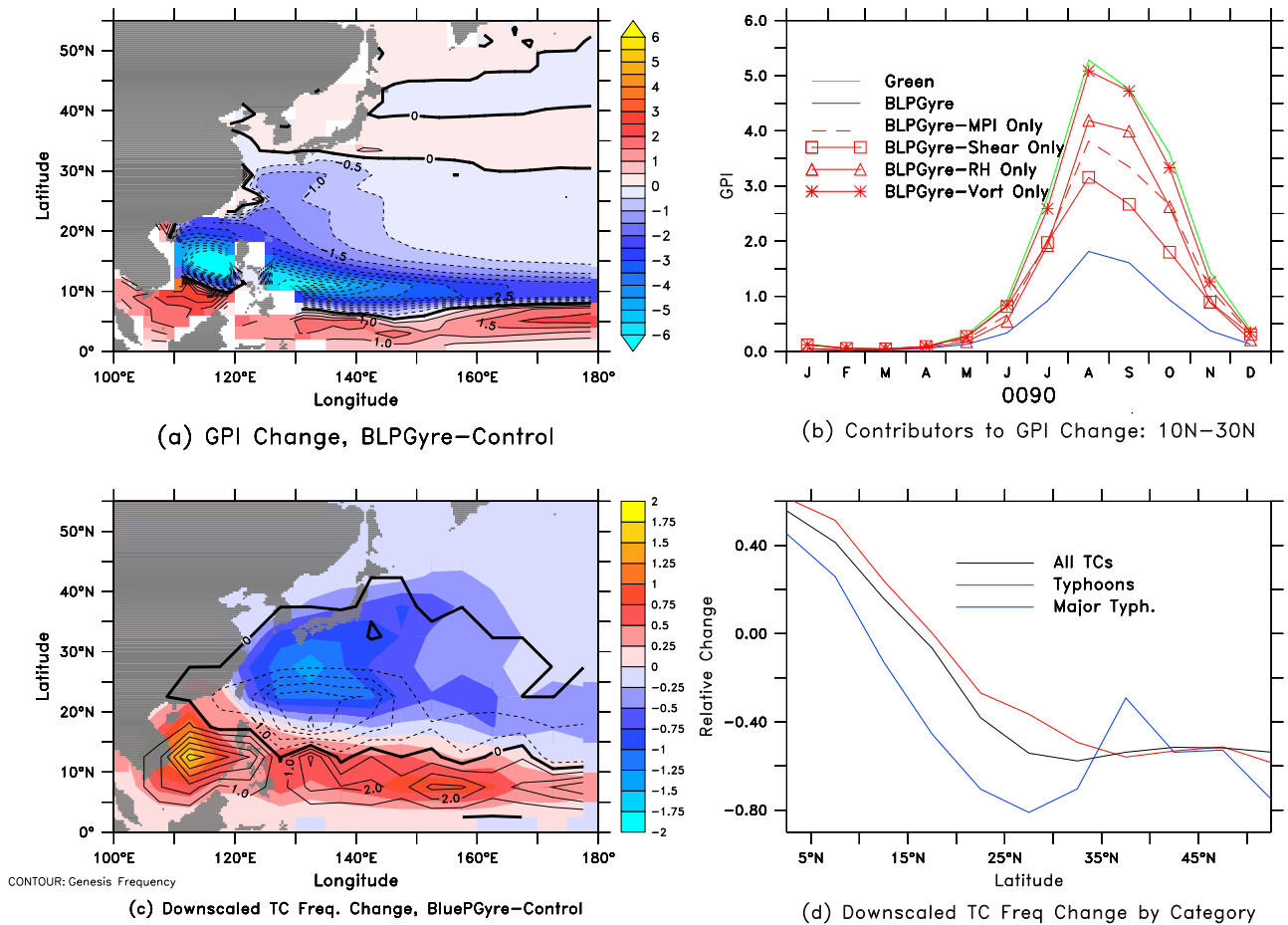
(a) GPI Change, BLPGyre−Control

(b) Contributors to GPI Change: 10N−30N

(c) Downscaled TC Freq. Change, BluePGyre−Control

(d) Downscaled TC Freq Change by Category

Figure 3. Changes in TC activity BLPGyre-Control. (a) Change in GPI. (b) Contributors to the change in GPI from 120W-180W, 10N-30N. (c) Difference in TC frequency (colors) and genesis frequency (contours) from statistical-dynamical downscale. (d) Relative change in TC frequency as a function of latitude for differing storm magnitudes from statistical-dynamical downscale. "Typhoons" refer to storms with winds >33m/s. "Major typhoons" have winds >49 m/s.

is well-correlated with SST anomalies in the NINO3 region in the BLPGyre model, with more La Nina-like conditions giving fewer storms in the West Pacific in accordance with observations. However as the BLPGyre run never enters the La Nina state as defined according to SST in the Green run, it would be expected to have *more* storms. Instead, there are generally fewer storms each year in the BLPGyre run (15% overall). Although the Green control does also experience
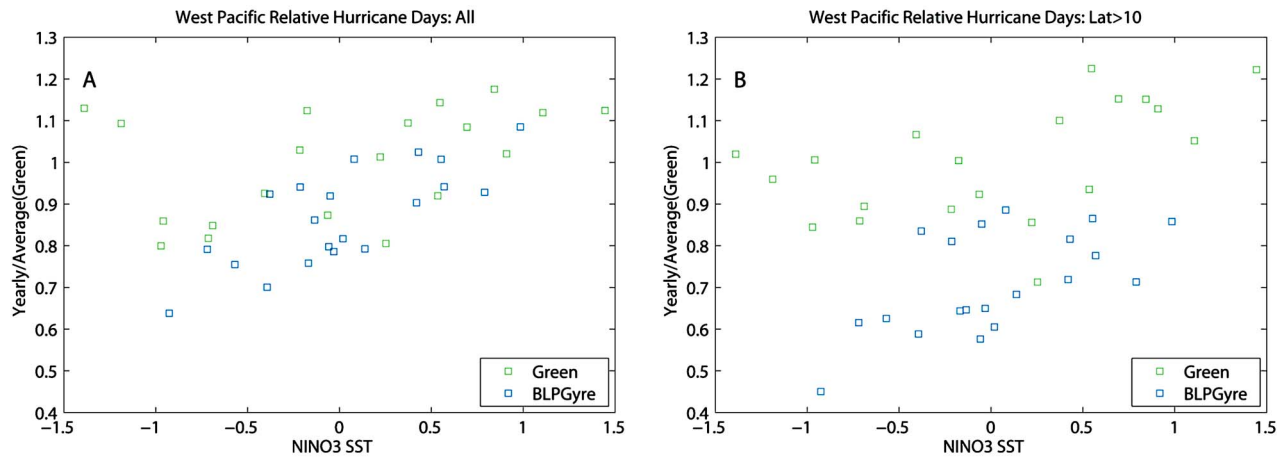

Figure 4. Relationship between NINO3 SST anomalies and typhoon activity (defined in terms of Relative Number of Hurricane Days = Hurricane Days for a given year/Mean hurricane days for Green control) calculated using statistical-dynamical downscaling. (a) All of Northwest Pacific (b) Northwest Pacific poleward of 10N.

two relatively active typhoon seasons during the very strongest La Nina years, the 20% enhancement during these two years is only sufficient to explain a 2% increase in typhoon frequency in the Green run relative to BLPGyre. When the region poleward of 15 degrees is considered (Figure 4b), the difference between the BLPGyre and Green runs is much larger (hurricane days drop by 43%). Although NINO3 SSTs are weakly correlated with hurricane days polewards of 15N (0.33 for Green, 0.44 for BLPGyre), the key driver of change is clearly the difference in the mean state, not the variability.

4. Discussion and Conclusions

[16] The presence of light-absorbing material substantially shapes the paths of Pacific TCs, allowing them to propagate to higher latitudes. While removing all excess absorbing materials is obviously extreme, there is evidence [*Karl et al.*, 2001] that during the 1960s chlorophyll levels in Pacific subtropical gyres were 50% lower than at present-although it is unclear how much of the change is due to differences in measurement techniques. In our Half run, the resulting atmosphere produces a GPI about 35% lower in the subtropical NW Pacific, about half the drop seen in Figure 3a. As this reduction in cyclone frequency is consistent with lower cyclone activity during the 1960s it raises the question of whether ocean color acted either to explain some part of the change or to amplify the impacts of larger-scale climate variability. However, in the absence of a clear mechanism for changing ocean chlorophyll during this time period, it would be premature to attribute the change in cyclone activity to any such mechanism.

[17] Additionally our results suggest that climate modelers wishing to make statements about tropical cyclones need to be extremely careful in describing the physics of the upper ocean. A separate set of experiments using a descendant of the coupled model used here (described in the Supplementary Materials) show that changing the details of the shortwave absorption parameterization can also produce significant changes in the distribution of TCs, though in this case primarily in the Northeast Pacific. This also highlights the importance of characterizing both shortwave absorption and turbulent mixing in the upper thermocline of the tropical oceans, if future estimates of TC activity are to be well-constrained.

References

Anderson, W. G., A. Gnanadesikan, R. Hallberg, J. Dunne, and B. L. Samuels (2007), Impact of ocean color on the maintenance of the Pacific Cold Tongue, *Geophys. Res. Lett.*, 34, L11609, doi:10.1029/2007GL030100.

Anderson, W. G., A. Gnanadesikan, and A. T. Wittenberg (2009), Regional impacts of ocean color on tropical Pacific variability, *Ocean Sci.*, 5, 313–327, doi:10.5194/os-5-313-2009.

Camargo, S., K. Emanuel, and A. H. Sobel (2007), Use of a genesis potential index to diagnose ENSO effects on tropical cyclone genesis, *J. Clim.*, 20, 4819–4833, doi:10.1175/JCLI4282.1.

Camargo, S., M. C. Wheeler, and A. H. Sobel (2009), Diagnosis of the MJO modulation of tropical cyclogenesis using an empirical index, *J. Atmos. Sci.*, 66, 3061–3074, doi:10.1175/2009JAS3101.1.

Chan, J. C. L. (1985), Tropical cyclone activity in the northwest Pacific in relation to the El Niño Southern Oscillation phenomenon, *Mon. Weather Rev.*, 113, 599–606, doi:10.1175/1520-0493(1985)113<0599:TCAITN>2.0.CO;2.

Delworth, T., et al. (2006), GFDL's CM2 global coupled climate models. Part 1: Formulation and simulation characteristics, *J. Clim.*, 19, 643–674, doi:10.1175/JCLI3629.1.

Emanuel, K. (1986), An air-sea interaction theory for tropical cyclones. Part I: Steady-state maintenance, *J. Atmos. Sci.*, 43, 585–605, doi:10.1175/1520-0469(1986)043<0585:AASITF>2.0.CO;2.

Emanuel, K. (2006), Climate and tropical cyclone activity: A model downscaling approach, *J. Clim.*, 19, 4797–4802, doi:10.1175/JCLI3908.1.

Gnanadesikan, A., and W. G. Anderson (2009), Ocean water clarity and the ocean general circulation in a coupled climate model, *J. Phys. Oceanogr.*, 39, 314–332, doi:10.1175/2008JPO3935.1.

Griffies, S. M., R. C. Pacanowski, and R. W. Hallberg (2000), Spurious diapycnal mixing associated with advection in a z-coordinate model, *Mon. Weather Rev.*, 128, 538–564, doi:10.1175/1520-0493(2000)128<0538:SDMAWA>2.0.CO;2.

Hallberg, R., and A. Gnanadesikan (2006), The role of eddies in determining the structure and response of the wind-driven Southern Hemisphere overturning: Results from the Modeling Eddies in the Southern Ocean (MESO) project, *J. Phys. Oceanogr.*, 36, 2232–2252, doi:10.1175/JPO2980.1.

Jerlov, N. G. (1968), *Optical Oceanography, Elsevier Oceanogr. Ser.*, 5, 194 pp.

Karl, D. M., R. R. Bidigare, and R. M. Letelier (2001), Long-term changes in phytoplankton community structure and productivity in the North Pacific Subtropical Gyre: The domain shift hypothesis, *Deep Sea Res., Part II*, 48, 1449–1470, doi:10.1016/S0967-0645(00)00149-1.

Lengaigne, M., et al. (2007), Influence of the oceanic biology on the tropical Pacific climate in a coupled general circulation model, *Clim. Dyn.*, 28, 503–516, doi:10.1007/s00382-006-0200-2.

Lewis, M. R., M. E. Carr, G. C. Feldman, W. Esaias, and C. McClain (1990), Influence of penetrating solar radiation on the heat budget of the equatorial Pacific Ocean, *Nature*, 347, 543–545, doi:10.1038/347543a0.

Manizza, M., C. Le Quere, A. J. Watson, and E. T. Buitenhuis (2005), Bio-optical feedbacks among phytoplankton, upper ocean physics and sea ice in a global model, *Geophys. Res. Lett.*, 32, L05603, doi:10.1029/2004GL020778.

Maue, R. N. (2009), Northern Hemisphere tropical cyclone activity, *Geophys. Res. Lett.*, 36, L05805, doi:10.1029/2008GL035946.

Morel, A. (1988), Optical modeling of the upper ocean in relation to its biogenous matter content (case I waters), *J. Geophys. Res.*, 93, 10,749–10,768, doi:10.1029/JC093iC09p10749.

Nakamoto, S., S. P. Kumar, J. M. Oberhuber, J. Ishizaka, K. Muneyama, and R. Frouin (2001), Response of the equatorial Pacific to chlorophyll pigment in a mixed layer isopycnal ocean general circulation model, *Geophys. Res. Lett.*, 28, 2021–2024, doi:10.1029/2000GL012494.

Reichler, T., and J. Kim (2008), How well do coupled climate models simulate today's climate, *Bull. Am. Meteorol. Soc.*, 89, 303–311, doi:10.1175/BAMS-89-3-303.

Saunders, M. A., R. E. Chandler, C. J. Merchant, and F. P. Roberts (2000), Atlantic Hurricanes and NW Pacific typhoons: ENSO spatial impacts on occurrence and landfall, *Geophys. Res. Lett.*, 27, 1147–1150, doi:10.1029/1999GL010948.

Schultz, P. (2008) Observing phytoplankton physiology and ecosystem structure from space, Ph.D. thesis, 245 pp., Princeton Univ., Princeton, N. J.

Sweeney, C., A. Gnanadesikan, S. M. Griffies, M. J. Harrison, A. Rosati, and B. L. Samuels (2005), Impacts of shortwave penetration depth on large-scale ocean-circulation and heat transport, *J. Phys. Oceanogr.*, 35, 1103–1119, doi:10.1175/JPO2740.1.

Vecchi, G. A., and B. J. Soden (2007), Increased Atlantic wind shear in projections of global warming, *Geophys. Res. Lett.*, 34, L08702, doi:10.1029/2006GL028905.

Yoder, J. A., and M. A. Kennelly (2003), Seasonal and ENSO variability in global ocean phytoplankton chlorophyll derived from 4 years of SeaWiFS measurements, *Global Biogeochem. Cycles*, 17(4), 1112, doi:10.1029/2002GB001942.

Zhao, M., I. Held, S.-J. Lin, and G. A. Vecchi (2009), Simulations of global hurricane climatology, interannual variability and response to global warming using a 50km resolution GCM, *J. Clim.*, 22, 6653–6678, doi:10.1175/2009JCLI3049.1.

W. G. Anderson, A. Gnanadesikan, R. Hallberg, and G. A. Vecchi, Geophysical Fluid Dynamics Laboratory, NOAA, 201 Forrestal Rd., Princeton, NJ 08540, USA. (anand.gnanadesikan@noaa.gov)

K. Emanuel, Department of Earth, Atmosphere and Planetary Sciences, Massachusetts Institute of Technology, 77 Massachusetts Ave., Room 54-1620, Cambridge, MA 02139, USA.